BRG1 promotes transcriptional patterns that are permissive to proliferation in cancer cells

Authors:

Katherine A. Giles[1,2,3], Cathryn M. Gould[1], Joanna Achinger-Kawecka[1,4], Scott G. Page[2], Georgia Kafer[2], Phuc-Loi Luu[1,4], Anthony J. Cesare[2], Susan J. Clark[1,4]*, Phillippa C. Taberlay[3]*

*These authors contributed equally

Affiliations:

[1]Epigenetics Research Laboratory, Genomics & Epigenetics Theme, Garvan Institute of Medical Research, Sydney, NSW, 2010, Australia

[2]Genome Integrity Unit, Children's Medical Research Institute, University of Sydney, Westmead, NSW, 2145, Australia

[3]School of Medicine, College of Health and Medicine, University of Tasmania, Hobart, TAS, 7000, Australia

[4]St Vincent's Clinical School, UNSW Sydney, Sydney, NSW, 2000, Australia

Correspondence: Phillippa C. Taberlay (phillippa.taberlay@utas.edu.au)

Running Title: BRG1 links transcription and proliferation

Keywords: BRG1, *SMARCA4*, chromatin remodelling, cancer, gene expression, cell cycle, transcription, replication

ABSTRACT

Deregulated expression of the chromatin remodeller, BRG1 (Brahma related gene 1; encoded by *SMARCA4*), is observed in a wide range of malignancies. Yet, the underlying function and cellular consequences of altered BRG1 expression during oncogenesis are still being uncovered. Here, we have investigated a role for BRG1 in directing genome-wide transcription programs in the context of prostate cancer. We examined The Cancer Genome Atlas (TCGA) prostate cancer cohort and a panel of prostate cell lines and found *SMARCA4* was consistently overexpressed irrespective of Gleason grade or molecular subtype. We then tested the effect of BRG1 depletion on transcriptional patterns in LNCaP prostate cancer cells. This revealed BRG1 depletion does not impact alternative splicing and surprisingly, confers only a modest effect on global gene expression. Of the transcriptional changes that did occur, most manifested as down-regulated gene expression with striking enrichment of multiple genes involved in cell cycle progression, and those that have previously been associated with prostate cancer proliferation. We found BRG1 regulated genes could be defined by the presence or absence of AR and FOXA1 occupancy at their cognate gene promoters. Genes co-regulated by BRG1, AR and FOXA1 include known prostate cancer genes *KLK2*, *PCAT1* and *VAV3*. Genes regulated by BRG1 independently of AR and FOXA1 include several proliferation and DNA replication factors. In agreement with the transcriptional changes, depleting BRG1 conferred G1 arrest. Together, these data show that BRG1 regulates transcription of proliferative and oncogenic factors, providing mechanistic insight into the function of BRG1 in prostate cancer cells.

INTRODUCTION

Nucleosomes serve as a physical backbone for chromatin organization both on a global scale and at local gene regulatory elements. Nucleosomes therefore govern both genome-wide stability and local DNA accessibility (Giles and Taberlay 2019b). Nucleosome positioning by ATP-dependent chromatin remodellers play a critical role in regulating DNA accessibility, allowing genes to be expressed at the appropriate place and time (Giles and Taberlay 2019b). Genomic profiling has demonstrated that dynamic regulation of DNA accessibility loci occurs primarily at DNA regulatory elements, which are cell type specific, and that DNA accessibility changes reflect concomitant transcriptional patterns. (Thurman et al. 2012; Taberlay et al. 2014). It is essential for chromatin to be relaxed at active gene promoters to create an ordered nucleosome disassembly, which permits binding of RNA pol II and the general transcription machinery (Heintzman et al. 2007; Skulte et al. 2014). In agreement, ChIP-seq data has revealed that transcription factors are concentrated on accessible DNA, with the highest levels of bound transcription factors correlating with the most accessible genomic regions (Li et al. 2011). Conversely, chromatin condensation resulting in reduced DNA accessibility is necessary for transcriptional repression (Venkatesh and Workman 2015). Disruption to the DNA accessibility landscape is a feature of cancer (Taberlay et al. 2014; Makova and Hardison 2015; Taberlay et al. 2016). This was recently emphasized in genomic sequencing data from multiple cancers and cancer subtypes, which revealed associations between the accessible chromatin organization and mutation load (Makova and Hardison 2015). Moreover, studies of aged human and yeast cells demonstrated that nucleosome loss compromises genome stability, gene regulation and transcription (O'Sullivan et al. 2010; Hu et al. 2014).

Genes encoding ATP-dependent chromatin remodellers are themselves frequently mutated and often atypically expressed in cancer (Reisman et al. 2009; Wilson and Roberts 2011; Shain and

Pollack 2013; Skulte et al. 2014; Chu et al. 2017; Giles and Taberlay 2019a). Notably, the SWI/SNF chromatin remodelling complex is mutated or transcriptionally deregulated in ~20% of cancers; a mutation frequency approaching that of *TP53* (~26%) (Kadoch et al. 2013; Shain and Pollack 2013; Giles and Taberlay 2019a). The SWI/SNF complex is often described as a tumour suppressor because it is required by the Retinoblastoma protein (Rb) family for regulation of normal cell growth (Dunaief et al. 1994; Strober et al. 1996). Disruptions of multiple SWI/SNF subunits are reported in human tumours and cell lines (Wong et al. 2000; Medina et al. 2008; Reisman et al. 2009; Roberts and Biegel 2009; Wilson and Roberts 2011; Katagiri et al. 2012; You and Jones 2012; Bai et al. 2013; Bosse et al. 2013; Cho et al. 2013; Mao et al. 2013; Oike et al. 2013a; Romero et al. 2013; Shain and Pollack 2013; Shi et al. 2013; Yan et al. 2013; Buscarlet et al. 2014; Roy et al. 2014; Song et al. 2014; Yokoyama et al. 2014; Zhao et al. 2014), often accompanied by a loss of heterozygosity consistent with the inactivation of a tumour suppressor (Reisman et al. 2009; Roy et al. 2014). The specific SWI/SNF mutations observed in tumours and the cancers associated with altered SWI/SNF function have been extensively reviewed (Roberts and Orkin 2004; Reisman et al. 2009; Wilson and Roberts 2011; You and Jones 2012; Oike et al. 2013a; Shain and Pollack 2013; Roy et al. 2014; Giles and Taberlay 2019a). However, the mechanism and functional consequences have not been fully defined.

Brahma-related gene 1 (BRG1) is one of the two mutually exclusive ATPases within the SWI/SNF complex. BRG1 has known roles in regulating DNA for temporal gene expression at both promoters and enhancer gene regulatory elements (Heintzman et al. 2007; Hu et al. 2011; Tolstorukov et al. 2013; Bao et al. 2015; Alver et al. 2017; Hodges et al. 2018; Giles et al. 2019). Moreover, BRG1 plays a role in maintaining the epigenetic landscape of a cell at these gene regulatory elements. Specifically, BRG1 has been directly linked to transcriptional output through its recognition of H3K14ac (Shen et al. 2007; Luebben et al. 2010; Morrison et al. 2017). In the absence of H3K14ac, BRG1 is still present at promoters and histones are

disassembled from the chromatin; however, transcription is reduced (Church et al. 2017). At enhancers, BRG1 depletion greatly reduces H3K27ac and subtlety reduces H3K4me1, which is correlated with a decrease in chromatin accessibility (Hodges et al. 2018). BRG1 is also known to mediate inter-chromosomal looping interactions between specific loci such as the *MYC* enhancer and promoter, the alpha-globulin genes, the *IgH* locus, and the class II major histocompatibility complex gene locus (Ni et al. 2008; Kim et al. 2009a; Kim et al. 2009b; Shi et al. 2013; Bossen et al. 2015). On a global scale, BRG1 binding has been found at DNA-loop anchors (Giles et al. 2019) and topological associated domain (TAD) boundaries where it increases their stability (Barutcu et al. 2016). Together, this demonstrates an important role for BRG1 in maintaining chromatin for transcription regulation.

Interestingly, *SMARCA4*, the gene encoding BRG1, has been observed in both down- and up-regulated states in cancer, indicative of the diverse and complex BRG1 functions. *SMARCA4* mRNA was seen to be down regulated in bladder, colon, non-triple negative breast cancers, head and neck, oesophageal, melanoma, pancreatic, lung and ovarian cancers, and *SMARCA4* mutation rates in these cancers have been reported between 4-13% (Reisman et al. 2009; Bai et al. 2013; Shain and Pollack 2013; Shi et al. 2013; Buscarlet et al. 2014; Wilson et al. 2014; Agaimy et al. 2017; Herpel et al. 2017; Giles and Taberlay 2019a). In contrast, *SMARCA4* has been reported as over expressed in cancers of the prostate, triple negative breast cancers and some leukaemias (Sun et al. 2007; Bai et al. 2013; Shi et al. 2013; Buscarlet et al. 2014; Ding et al. 2019; Giles and Taberlay 2019a). In *SMARCA4* over expressing cancers, no significant recurrent mutations have been reported (Valdman et al. 2003; Li et al. 2006; Sun et al. 2007; Liu et al. 2010). The importance of BRG1 in cancer is further evidenced through studies of synthetic lethality, where BRG1 was observed to have a synthetic lethal relationship with the alternative SWI/SNF ATPase Braham (BRM), and Aurora A kinase in lung cancer, and PTEN in prostate cancer (Oike et al. 2013b; Tagal et al. 2017; Ding et al. 2019).

Examination of multiple prostate cancer cohorts has demonstrated elevated *SMARCA4* expression or increased BRG1 protein levels. Clinical studies of primary prostate tumours reported an overall increase in BRG1 protein by immunohistochemistry (Valdman et al. 2003; Li et al. 2006; Sun et al. 2007; Liu et al. 2010). Moreover, increased *SMARCA4* gene expression has been reported in RNA-seq data from The Cancer Genome Atlas (TCGA) prostate cancer cohort (Cancer Genome Atlas Research 2015; Muthuswami et al. 2019). While it is established that BRG1 is commonly up regulated in prostate cancer, the full range of molecular pathways impacted by dysregulated BRG1 levels and the contribution of these molecular changes to the atypical phenotype of prostate cancer cells remains unclear.

Here we dissected the molecular role of BRG1 on the transcriptome in prostate cancer. We confirmed that *SMARCA4* is over-expressed in prostate cancer irrespective of severity or cancer subtype and identified *SMARCA4* was also over expressed in a panel of prostate cancer cell lines. Depletion of BRG1 in LNCaP prostate cancer cells resulted in a modest effect on global gene transcription with the majority of changes resulting in down-regulated gene expression. Within the cohort of down-regulated genes in BRG1 depleted cells we identified gene clusters defined by their co-occupancy or independence from transcription factors AR and FOXA1, both of which are known BRG1 co-activators (Marshall et al. 2003; Dai et al. 2008; Hoffman et al. 2018). Our data revealed that BRG1, AR and FOXA1 co-regulate known prostate cancer genes *KLK2*, *PCAT1* and *VAV3*. Gene ontology analysis further revealed that genes regulated by BRG1 independent of AR and FOXA1 include factors regulating cell cycle and proliferation processes including DNA replication. In agreement, depleting BRG1 promoted G1 arrest resulting in reduced cell proliferation. Cumulatively the data indicate BRG1 promotes expression of cellular proliferation factors and cancer-associated genes in prostate cancer cells.

RESULTS

SMARCA4 is over expressed in prostate cancer irrespective of tumour grade or subtype

We first examined the TCGA (Cancer Genome Atlas Research 2015) prostate normal and cancer cohort. In agreement with previous findings (Muthuswami et al. 2019), we confirmed *SMARCA4* is up regulated in prostate tumours ($p<0.001$; Figure 1A) and that the increased expression is consistent for all Gleason score groups (Figure 1B). We also noted there was no significant difference in *SMARCA4* expression between each Gleason score group suggesting that over expression of *SMARCA4* is independent of tumour severity ($p<0.001$). We next analysed the data by dividing the patients into the seven molecular subtypes for prostate cancer, as categorised by TCGA (Cancer Genome Atlas Research 2015). The molecular subtypes include those with fusion genes involving *ERG* (46%), *ETV1* (8%), *ETV4* (4%) and *FLI1* (1%), or those with mutations in *SPOP* (11%), *FOXA1* (3%) or *IDH1* (1%) (Cancer Genome Atlas Research 2015). The remaining samples were grouped as 'other' (26%). Similar to Gleason score, each subtype exhibited a statistically significant increase in *SMARCA4* expression ($p<0.05$) with the exception of the 'FLI1' subtype ($p=0.5899$) and 'other' ($p=0.1899$), which both demonstrated a non-significant increase in *SMARCA4* expression (Figure 1C). Together, these data confirm that *SMARCA4* over expression is a common feature associated with prostate cancer irrespective of Gleason score or molecular subtype.

FIGURE 1

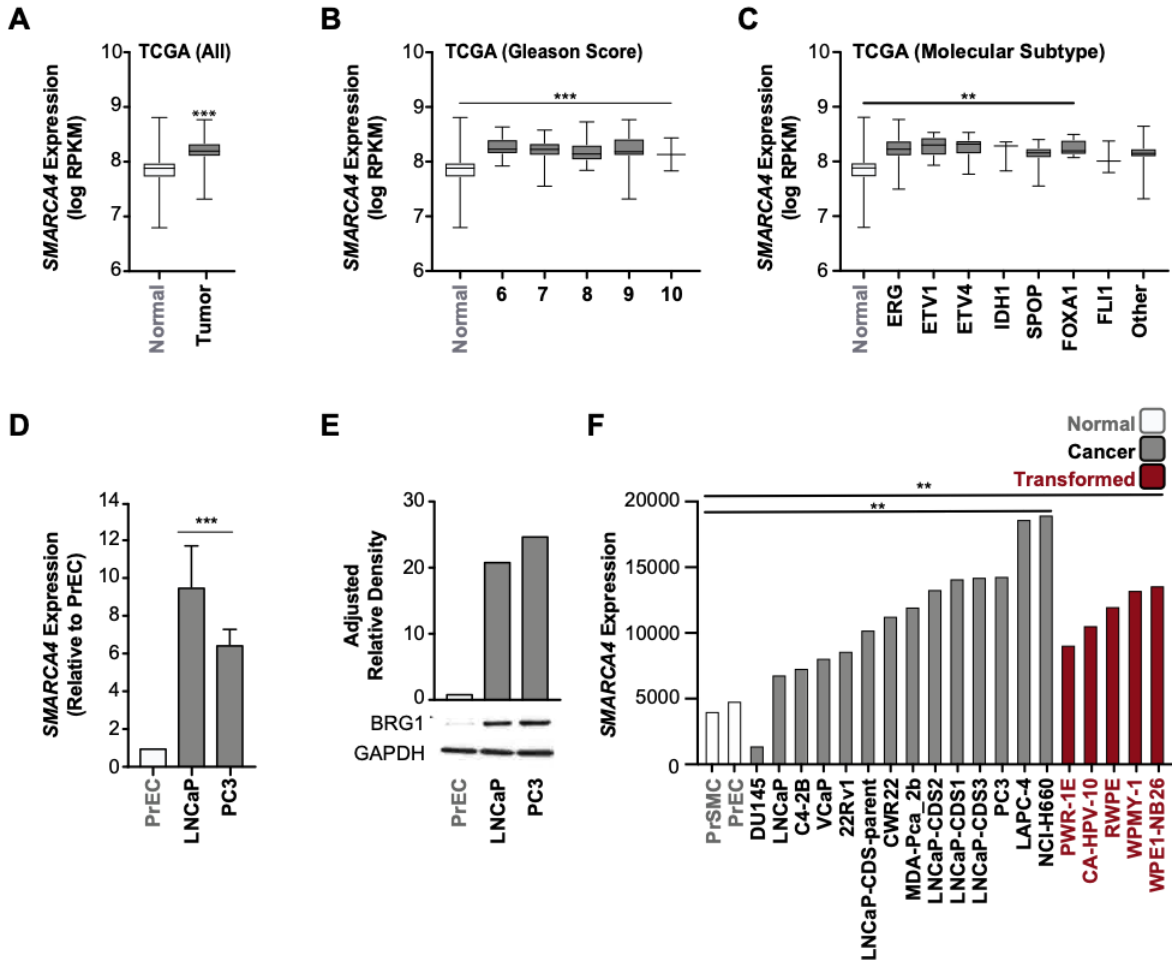

Figure 1. *SMARCA4* (BRG1) is over expressed in prostate cancer. A) *SMARCA4* gene expression (logRPKM) of all TCGA normal (n = 52) and cancer (n = 486) prostate samples. *SMARCA4* is significantly increased in the prostate tumour samples, unpaired T-test ****p<0.001*. B) *SMARCA4* gene expression (logRPKM) in TCGA data with tumour samples separated by Gleason score. *SMARCA4* expression in all Gleason score groups is significantly up regulated compared to the normal prostate samples, one-way ANOVA with Dunnett's multiple comparison correction ****p<0.001*. C) *SMARCA4* gene expression (logPRKM) in TCGA data with tumour samples separated by molecular subtype defined by the TCGA. *SMARCA4* expression is increased across all groups, with subtypes ERG, ETV1, ETV4, IDH1, SPOP, and FOXA1 all significantly up regulated, one-way ANOVA Dunnett's multiple comparison correction ***p<0.05*. D) *SMARCA4* gene expression in prostate cell lines normalised to 18s and

relative to PrEC (n = 2). Significance determined by one-way ANOVA with Tukey's multiple comparison correction ***$p<0.001$. E) Representative Western blot of BRG1 protein level in prostate cell lines quantified by adjusted relative density normalized to GAPDH and relative to PrEC. F) Expression of *SMARCA4* in prostate cell lines grouped as normal, cancer or transformed. The mean of each group was calculated, and a significance was tested by one-way ANOVA Dunnett's multiple comparison correction, **$p<0.05$.

SMARCA4 is over expressed in prostate cancer and transformed prostate cell lines

We next examined both BRG1 protein and *SMARCA4* gene expression levels in normal prostate epithelial cells (PrEC) and compared to LNCaP (lymph node metastasis), an androgen-dependent prostate cancer cell line, as well as PC3 (bone metastasis), an androgen-independent prostate cancer cell line. We found that *SMARCA4* gene expression was increased ~9 fold in LNCaP cells and ~6 fold in PC3 compared to PrEC ($p<0.001$; Figure 1D). Further, the BRG1 protein level was increased ~20 and ~24 fold, respectively, in each of the prostate cancer cell lines compared to PrEC (Figure 1E). We compared this to published RNA-seq data of several normal, cancer and transformed prostate cell lines (Prensner et al. 2011). The mean expression of *SMARCA4* was significantly increased in both the cancer cell lines and the transformed cell lines compared to the normal cells ($p=0.0148$ and $p=0.0353$ respectively; Figure 1F). The exception to this was DU145 cells that have a known frameshift mutation in *SMARCA4*, resulting in reduced expression (Wong et al. 2000). This data shows that common prostate cancer cell lines reflect the same pattern of increased BRG1 protein that is observed in prostate tumours compared to normal prostate samples and therefore provides an ideal model system to explore the functional consequences of BRG1 dysregulation on the transcriptome.

BRG1 is required for the maintenance of active gene expression

We depleted the level of BRG1 protein using two independent siRNAs targeting *SMARCA4* (si-

SMARCA4-1 and si-*SMARCA4*-2) and performed RNA-seq at 72 and 144 hours post transfection (Figure 2A). Initial assessment of our RNA-seq data confirmed successful depletion of the *SMARCA4* transcript (~80%) at both time points (Figure 2B). Additionally, we confirmed substantial depletion of BRG1 levels reduced to ~40% of the non-targeting control at 72 hours, and to ~20% of the non-targeting control at 144 hours post-transfection (Figure 2C). We note there were no significant changes detected in the gene expression of any other SWI/SNF subunit proteins (Supplementary Figure 1A). Further quality assessment of the RNA-seq data through a principal component analysis demonstrated that the samples separated by time-point on the first dimension, accounting for 43.39 % of the sample variance (Supplementary Figure 1B). We performed a differential gene expression analysis and identified 169 down-regulated genes and 24 up-regulated genes (logFC > 1.5, FDR < 0.05) at 72 hours post BRG1 depletion (Figure 2D). This increased to 800 down-regulated genes and 174 up-regulated genes by 144 hours post-transfection (Figure 2E). This suggests that the primary role of BRG1 in LNCaP cells is to maintain active gene expression of a subset of genes.

FIGURE 2

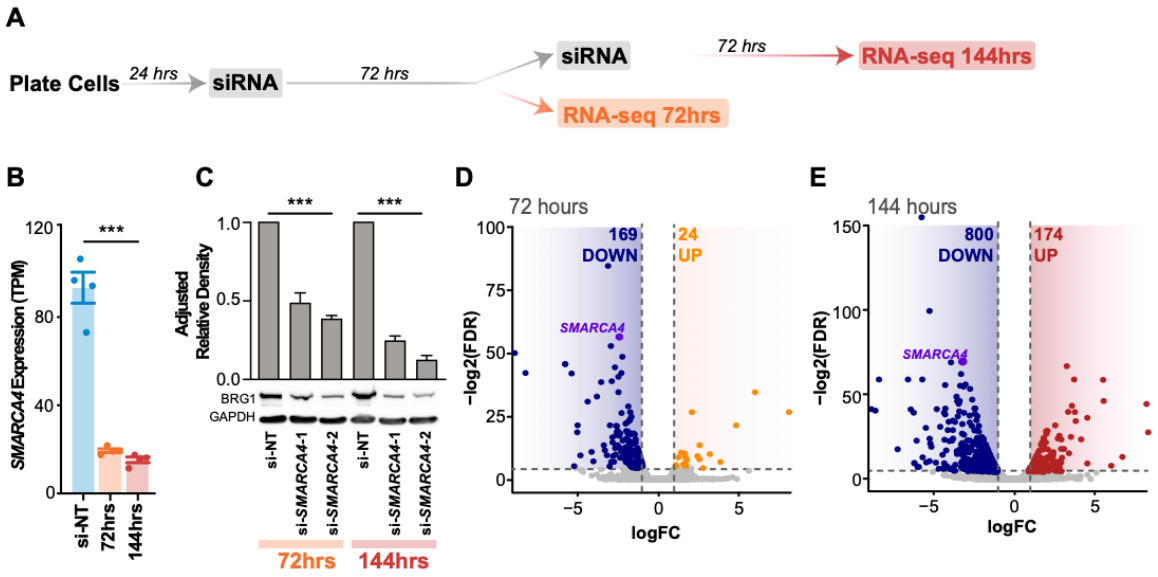

Figure 2. Loss of BRG1 results in a down regulation of gene expression. A) Schematic of temporal BRG1 knockdown model used for RNA-seq. B) *SMARCA4* gene expression from the RNA-seq datasets. Gene expression is shown as transcripts per million reads (TPM). *SMARCA4* expression is significantly down regulated at both time points, ****p<0.0001*. C) Representative Western blots of BRG1 and GAPDH protein levels at 72 and 144 hours post transfection. Adjusted relative density for BRG1 is calculated relative to GAPDH and normalized to the non-targeting control. D-E) Volcano plots of differentially expressed genes at 72 hours and 144 hours post knockdown. Significantly down regulated genes are blue and significantly up regulated genes for 72 and 144 hours post knockdown are shown in orange and red respectively. *SMARCA4* differential expression is highlighted in purple. Expression is shown as normalised log2 counts per million reads.

BRG1 does not play a role in the regulation of alternative splicing

The nucleosome barrier within genes is reported to contribute to alternative splicing, where there is a higher conservation of nucleosomes at the splice sites of constitutive exons compared to skipped exons (Andersson et al. 2009; Dhami et al. 2010; Huang et al. 2012). Since the contribution of BRG1 to alternative splicing regulation is unknown, we investigated if alterations in alternative splicing may explain down regulation of gene expression after BRG1 depletion in LNCaP cells. To do this we performed a multivariate analysis of transcript splicing (MATS; (Shen et al. 2012; Park et al. 2013; Shen et al. 2014)) of our RNA-seq datasets. After 72 hours of BRG1 depletion, MATS pairwise comparison detected a genome wide total of 13 and 11 skipped exons, and 14 and 9 retained introns with si-*SMARCA4*-1 and si-*SMARCA4*-2 respectively (Supplementary Figure 1C). At 144 hours post BRG1 knockdown this increased to 240 and 260 skipped exons, and 27 and 26 retained introns with si-*SMARCA4*-1 and si-*SMARCA4*-2, respectively (Supplementary Figure 1D). Given the relatively large number intron-exon junctions within the total LNCaP transcriptome, we conclude BRG1 does not extensively

contribute to alternative splicing as the mechanism for predominant gene down-regulation. However, we do note that at 144 hours post-knockdown the MATS analysis identified retention of the first intron from the Kallikrein 3 gene, which encodes prostate specific antigen (PSA) (Supplementary Figure 1E). This splice variant has previously been reported in LNCaP cells and generates a unique protein from canonical PSA (David et al. 2002). While PSA has a well-known link to prostate cancer, the function of it's alternative splice variant remains unknown.

BRG1 binding is associated with expression of prostate cancer associated genes

We further examined our RNA-seq datasets to determine which genes showed a significant change in expression at 72 hours that was maintained at 144 hours. Of the genes that were down-regulated at the 72 hour time point, 126 genes (75 %) remained down-regulated at 144 hours. Similarly, of the up-regulated genes, 16 (67 %) remained up-regulated at the extended time point (Figure 3A). Within the down-regulated gene set we note a number of genes that have previously been associated with increased proliferation in prostate cancer; these include kallikrein 2 (*KLK2*), long non-coding RNA prostate cancer associated transcript 1 (*PCAT1*), and Vav guanine nucleotide exchange factor 3 (*VAV3*) (Lyons and Burnstein 2006; Liu et al. 2008; Williams et al. 2010; Prensner et al. 2011; Lin et al. 2012; Rao et al. 2012; Prensner et al. 2014; Shang et al. 2014; Shang et al. 2019) (Figure 3B-D). We also examined the panel of prostate cell lines (Prensner et al. 2011) and confirmed that, on average there is elevated expression of these genes in both prostate cancer cells and transformed prostate cell lines compared to normal prostate cells (Supplementary Figure 2A). This suggests a role for BRG1 in maintaining the expression of genes associated with prostate cancer proliferation.

FIGURE 3

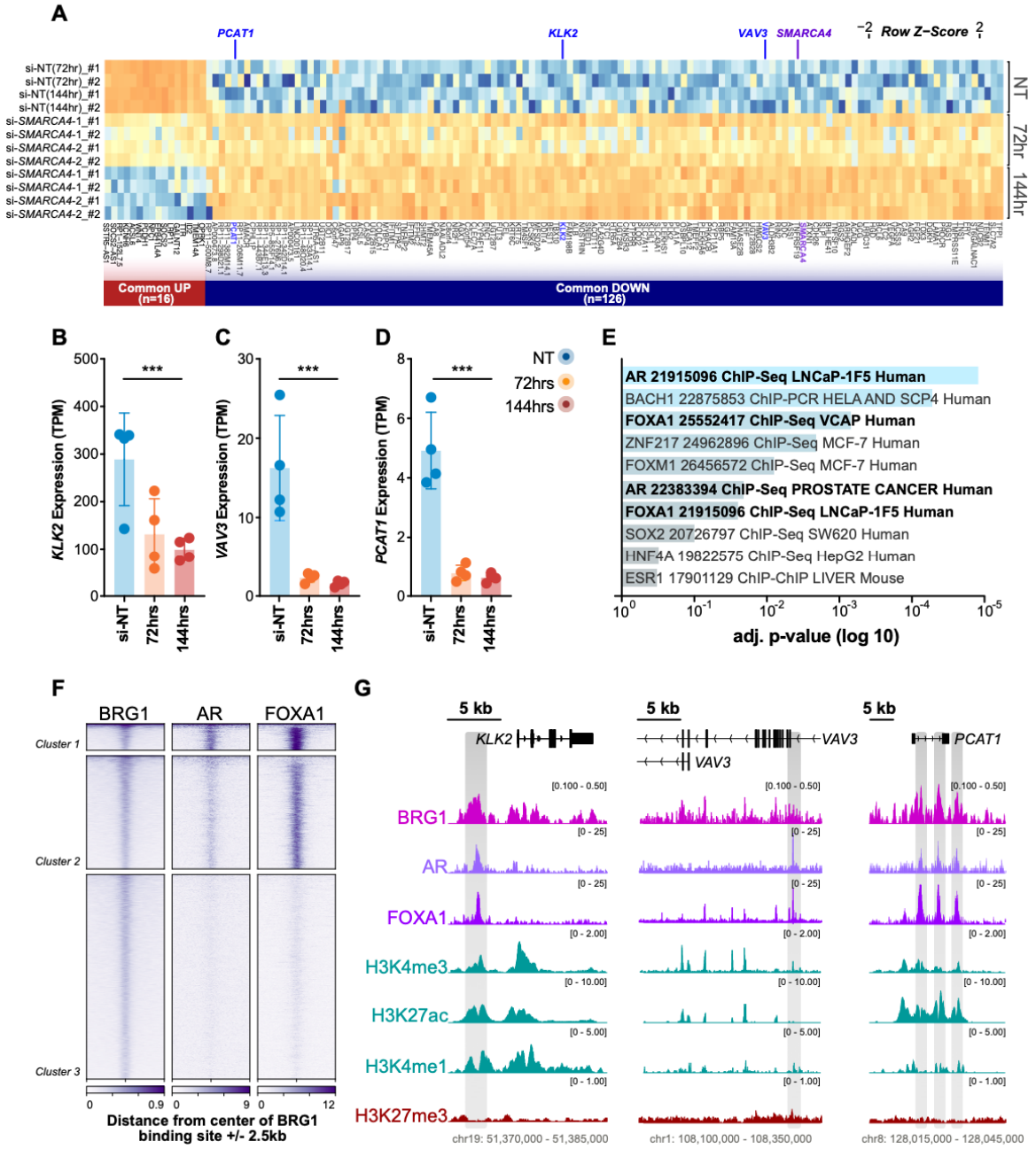

Figure 3. BRG1 regulates genes associated with prostate cancer. A) Heatmap illustrating RNA-seq differential gene expression data for up (n = 16) and down (n = 126) regulated genes common to both time points after BRG1 depletion. Expression is represented as the normalised row Z-score of TPM. B-D) *KLK2, VAV3 and PCAT-1* gene expression from the RNA-seq datasets shown as TPM. E) Gene set enrichment analysis using 'Enrichr' of differentially expressed genes that are common to both time points, showing the adjusted p-value (log 10,

reversed x-axis) of significantly enriched transcription factor ChIP-seq from ChEA curated data *($p<0.05$)*. F) Heatmap of BRG1, AR and FOXA1 ChIP-seq signal at BRG1 binding sites in LNCaP cells, +/- 2.5 kb from the centre of the binding site. Data is clustered into three groups by k-means. G) IGV images of the genes *KLK2*, *PCAT-1* and *VAV3*. Grey shaded regions contain ChIP-seq signal peaks for BRG1, AR and FOXA1.

We next sought to further explore commonalities in the genes with a significant change in expression at both time points. We used 'Enrichr' (Chen et al. 2013; Kuleshov et al. 2016) to determine which existing ChIP-seq datasets of transcription factors had enriched binding at the promoters of these genes. We discovered that the most significantly enriched datasets were for the androgen receptor (AR) and Forkhead box A1 (FOXA1) (Figure 3E), both of which are important for prostate cancer growth (Marshall et al. 2003; Dai et al. 2008; Andreu-Vieyra et al. 2011; Chen et al. 2015; Jones et al. 2015; Ye et al. 2016; Gui et al. 2019). To investigate the potential coordinated function of these transcription factors with BRG1, we compare the ChIP-seq signal of BRG1 (Ye et al. 2016), AR (Gui et al. 2019) and FOXA1 (Gui et al. 2019) at BRG1 genome-wide binding sites in LNCaP cells. We found the profiles separated into three clusters. Cluster 1 sites displayed strong AR and FOXA1 binding, cluster 2 had moderate AR and strong FOXA1, and cluster 3 had minimal to no signal for AR or FOXA1 (Figure 3F). We next examined the key BRG1 regulated genes *KLK2*, *PCAT1* and *VAV3*, and found coordinated binding of all three factors at the promoters of *KLK2* and *PCAT1*, and binding of BRG1 and FOXA1 upstream of the internal 3-prime promoter of *VAV3* (Figure 3G). Furthermore, we showed that the expression of AR or FOXA1 themselves was not regulated by BRG1 (Supplementary Figure 2B-C), suggesting that the loss of BRG1 is enough to disrupt expression and regulation of *KLK2*, *PCAT1* and *VAV3*.

BRG1 binding is associated with the expression of key DNA replication genes

As the majority of significant gene changes occurred at 144 hours post-knockdown, we next investigated potential gene regulatory networks. Gene ontology analysis with Enrichr (Chen et al. 2013; Kuleshov et al. 2016) identified several significant (FDR < 0.05) GO terms pertaining to biological processes, cellular component and molecular function that were all broadly related to the cell cycle (Figure 4A). As BRG1 has previously been shown to interact with cell cycle master regulators, such as Rb and p53 (Strober et al. 1996; Strobeck et al. 2000; Zhang et al. 2000; Naidu et al. 2009), we explored the relationship between the cell cycle and BRG1 further in our datasets. We compiled a list of 250 genes related to cell cycle processes, curated from the cell cycle GO terms, and of these examined the top 40 most significantly down-regulated genes in our dataset. Of note among the list were several key genes involved in DNA replication initiation such as *CDC6*, *CDT1* and *CDC45*, as well as the Minichromosome Maintenance (MCM) replicative helicase components *MCM2* and *MCM5* (Figure 4B). To investigate if the effect on replication initiation gene expression was more widespread, we reviewed the gene expression of the other components in the MCM2-7 replicative helicase and the Origin Recognition Complex (ORC) and found that several of these genes were also down-regulated (Figure 4C-D). We confirmed the down regulation of MCM5, CDC6 and ORC6 via Western blot, along with cell cycle regulator CHK1, which revealed almost undetectable expression by 144 hours post BRG1 knockdown (Figure 4E-F).

FIGURE 4

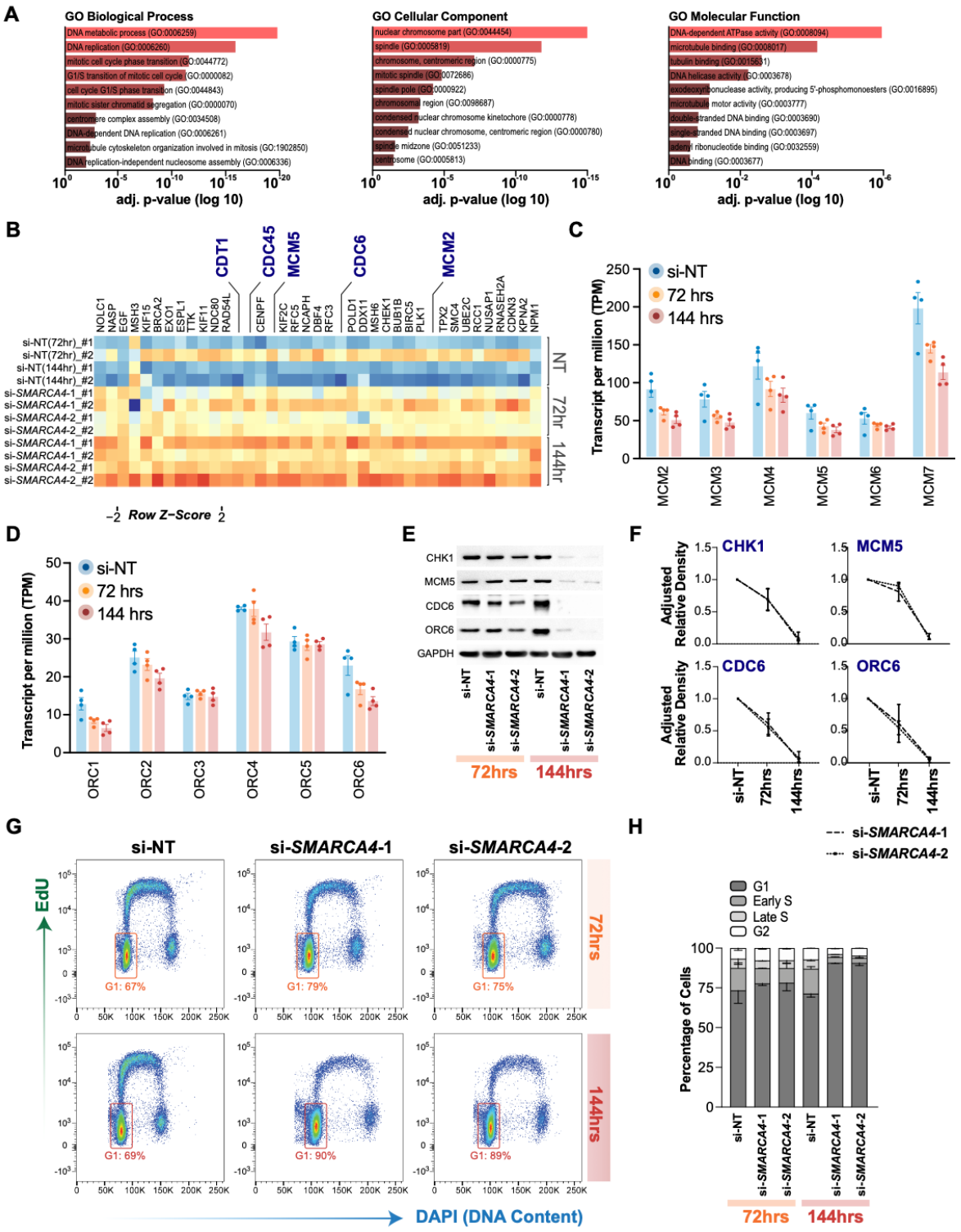

Figure 4. BRG1 regulates genes involved the cell cycle. A) Gene set enrichment analysis using 'Enrichr' of down regulated genes at 144 hours post BRG1 knockdown. Enriched GO terms are classified as biological processes, cellular component or molecular function. Adjusted p-value (log 10, reversed x-axis) of the 10 most significant GO terms are shown. B) Heatmap of gene

expression profiles from the top 40 differential cell cycle genes after BRG1 depletion. Expression is shown as the normalised row Z-score of transcripts per million reads (TPM), with blue indicating higher expression and red indicating lower expression. Genes involved in DNA replication initiation are indicated in blue. C-D) Gene expression from RNA-seq (TPM), of the MCM2-7 helicase components (top) and the Origin of Replication complex (ORC) subunits (bottom). Error bars denote mean and standard deviation. E) Representative Western blot showing protein levels of replication initiation genes MCM5, CDC6 and ORC6, along with CHK1, after 72 and 144 hours post BRG1 depletion. F) Quantification of Western blots demonstrating adjusted relative density to GAPDH (n = 2). G) Representative flow cytometry scatter of DAPI (x-axis) and EdU (y-axis) fluorescence intensity at 72 and 144 hours post BRG1 knockdown. G1 cells are shown by boxed gate. H) Percentage of cells in each phase of the cell cycle from flow cytometry data, error bars show standard deviation (n = 2).

We investigated whether AR and FOXA1 were also colocalised with BRG1 at DNA replication genes. We examined the ChIP-seq binding profiles of AR, FOXA1 and BRG1 at the promoters of 91 DNA replication genes (determined from the DNA replication GO terms) that were expressed in LNCaP cells. We found at promoters of these genes containing the active histone marks H3K4me3 and H3K27ac, also displayed a weak BRG1 ChIP-seq signal, but were completely absent of AR and FOXA1 ChIP-seq peaks (Supplementary Figure 3A), for example at the promoters of *CDC45*, *ORC6* (Supplementary Figure 3B. Additionally, we note also note this pattern at a putative enhancer region within the *MCM2* gene (Supplementary Figure 3B). Our data suggests that BRG1 binding is associated with the expression of DNA replication genes in prostate cancer cells that is independent of AR and FOXA1.

BRG1 depletion reduces cell proliferation and alters nuclei morphology

Given BRG1 regulates several genes involved in proliferation and replication, we next asked if

BRG1 depletion would alter cell cycle progression in LNCaP cells. We investigated this utilising the same siRNA-mediated approach to target BRG1 by depleting *SMARCA4* and conducted flow cytometry cell cycle analysis at 72 and 144 hours post knockdown. We detected an increase of cells in G1 at 72 hours, which was enhanced by 144 hours. Specifically, at 144 hours post BRG1 depletion there was ~20% increase of cells in G1 and equivalent loss of cells in S phase (Figure 4G-H). These data suggest that a loss of BRG1 reduces proliferation through mediating a G1 arrest.

DISCUSSION

This study has examined the involvement of the SWI/SNF chromatin remodeller BRG1 and its associated encoding gene *SMARCA4* in prostate cancer transcriptional deregulation. We found that over expression of *SMARCA4* commonly occurs in prostate cancer, irrespective of tumour grade or subtype. Using a temporal model to knockdown *SMARCA4* and consequently BRG1 protein in LNCaP prostate cancer cells, we found that BRG1 contributes to activation of a number of transcriptional pathways that promote proliferation. BRG1 regulates the active expression of genes already shown to play a role in the proliferation of prostate cancer. Depletion of BRG1 results in the down-regulation of cell cycle and DNA replication genes and results in G1 arrest. Taken together, our results provide new insights into BRG1's contribution to transcriptional patterns relating to proliferation in prostate cancer.

We have demonstrated that *SMARCA4* mRNA over expression is a general feature of prostate cancer. Clinical datasets have shown BRG1 protein levels are over-expressed in prostate cancer, in the absence of consistent significant deleterious genetic mutations evident in *SMARCA4* (Valdman et al. 2003; Li et al. 2006; Sun et al. 2007; Liu et al. 2010). Using the large prostate cancer cohort from TCGA (Cancer Genome Atlas Research 2015) we found that *SMARCA4* was

significantly over-expressed, in line with previous studies (Muthuswami et al. 2019). Consistent with this, *SMARCA4* expression was increased in a panel of both prostate cancer and transformed cell lines. However, unlike studies that focused on the protein level of BRG1 (Sun et al. 2007; Ding et al. 2019), we found no correlation between over-expression with Gleason grade at the RNA level, nor did we find a correlation between over-expression and tumour molecular subtype. These data emphasise that the overall increased expression of *SMARCA4* is a characteristic of prostate cancer, irrespective of subtype.

BRG1 depletion followed by RNA-seq revealed multiple transcriptomic alterations that were regulated by BRG1 and related to proliferation. Interestingly, BRG1 depletion tended to result in the down-regulation of BRG1's target genes, suggesting that the main role of BRG1 is to promote active gene expression. Within the down-regulated genes were genes associated with increased proliferation in prostate cancer including *KLK2*, *PCAT-1* and *VAV3*. KLK2 is a known activator of PSA, which is an important biomarker of prostate cancer, and associated with decreased apoptosis (Williams et al. 2010; Shang et al. 2014). *PCAT-1* promotes proliferation through the oncoprotein Myc (Prensner et al. 2011; Prensner et al. 2014), while VAV3 regulates AR activity to stimulate growth in prostate cancer (Lyons and Burnstein 2006; Liu et al. 2008; Lin et al. 2012; Rao et al. 2012), both of which are correlated with disease progression. Through an analysis of gene ontologies, we also found several cell cycle gene pathways were down-regulated. Notably, we observed that numerous genes involved in DNA replication were altered by BRG1 depletion, and these genes were among the most significantly down regulated. BRG1 has been shown to influence the expression of genes which regulate cell cycle progression (Rb, E2Fs, cyclins, Myc and p53) (Chi et al. 2003; Vicent et al. 2006; Ramirez-Carrozzi et al. 2009; Leung and Nevins 2012; Skulte et al. 2014; Velez-Cruz et al. 2016; Kaufmann et al. 2017; Vieira et al. 2017) and also have a role in driving self-renewal and malignancy in B-cell acute lymphoblastic and acute myeloid leukaemias (Shi et al. 2013; Buscarlet et al. 2014).

Specifically, these leukaemias require high levels of BRG1 for de-condensation of the cell specific *MYC* enhancer. In these cancers, a loss of BRG1 causes a reduction of enhancer-promoter interactions, reduced transcription factor occupancy and DNA looping which in turn reduces *MYC* expression (Shi et al. 2013). This implies that the overexpression of BRG1 contributes to driving oncogenic transcriptional programs which influence the proliferation capacity of cancer cells.

Our data revealed that BRG1 co-occupied the promotors of proliferation associated genes (*KLK2*, *PCAT-1* and *VAV3)* along with AR and FOXA1, and that these genes were down-regulated across our experimental time course. Co-regulation of transcription by AR and FOXA1 in prostate cancer is associated with reprogrammed binding of AR and oncogenic patterns of gene expression that are essential for AR-driven proliferation (Pomerantz et al. 2015; Stelloo et al. 2018). Additionally, there is a high overlap of these reprogrammed AR binding sites between LNCaP cells and primary prostate tumour tissue (Pomerantz et al. 2015). Here we have shown BRG1 gene regulation overlaps with these transcription factors at gene promoters, which is concomitant with expression of prostate cancer associated genes. However, it is also worth noting that we find that the manipulation of BRG1 expression also altered the expression of DNA replication genes, an effect which appears to be independent of AR and FOXA1. This data suggests that BRG1 has additional roles in other gene regulatory networks, which may indirectly influence cell proliferation. As BRG1 is known to interact with cell cycle regulators in other cancers, it is possible that genes co-regulated by BRG1, AR and FOXA1 are important in a prostate cancer context, while regulation of cell cycle and DNA replication genes may be a general feature of BRG1 over expression in cancer.

In summary, our data points to a fundamental role for BRG1 in maintaining active transcription for proliferation of prostate cancer cells. We find that BRG1 promotes gene expression in

prostate cancer models with varying degrees of dependence on AR and FOXA1. BRG1 is required to drive the expression of numerous prostate cancer specific genes in an AR/FOXA1 dependant manner, but also works independently to drive the expression of pro-proliferative and DNA replication genes. These results provide important functional information regarding the role of BRG1 controlling proliferation in prostate cancer cells.

METHODS

Cell Culture and siRNA Transfection

Normal Prostate Epithelial Cells (PrEC) cells (Cambrex Bio Science, #CC-2555) were cultured in PrEBM (Clonetics, #CC-3165) according to the manufacturer's protocol. Briefly, PrEC cells were seeded at 2,500 cells per cm^2 and medium was replaced every two days. Cells were passaged at approximately 80 % confluence. To passage a T75 flask, PrEC cells were rinsed in 6 mls Hanks Balanced Salt Solution (Thermo Fisher Scientific, #14025076) then detached with 2 ml pre-warmed 0.025 % Trypsin-EDTA and incubated at room temperature for 5 minutes. Trypsin was inactivated with 12 mls of Trypsin-Neutralizing Solution (Clonetics, #CC-5002) and cells were centrifuged at 300 x g for 5 minutes. The supernatant was aspirated, and the cell pellet was re-suspended in PrEBM. The number of cells was determined on the Countess automated counter and were re-seeded at the appropriate density based on experimental needs. Cells were discarded after ~16 population doublings.

PC3 cells (ATCC, #CRL-1435) were maintained in RPMI medium (Gibco, #11875-093) with 10 % FBS, 11 mls of 1 M HEPES (Gibco, #15630080) and Pen/Strep. LNCaP cells (ATCC, #CRL-1740) were cultured using custom T-Medium from Gibco (DMEM low glucose (GIBCO cat# 31600-034), Kaighn's modified F-12 medium (F-12K; cat# 211227-014), insulin 500x bovine pancreas (Sigma cat# I1882.10MG), T3 6.825 ng/ml Tri-iodothyronine (Sigma cat# T5516),

Transferrin 500x (Sigma cat# T5391), Biotin 500x (Sigma cat# B4639), Adenine 500x (Sigma cat# A3259)). Both prostate cell lines were cultured under recommend conditions; 37°C with 5 % CO_2. When the cells reached ~80 % confluence they were passaged or seeded as per experimental requirements. For siRNA transfection LNCaP cells were seeded into 6-well plates at a density of 2.5 x 10^5 cells per well or 10cm dishes at 1.5 x 10^6 cells per dish. The cells were transfected with either on target *SMARCA4* siRNA (Horizon, #J-010431-06-0005 or #J-010431-07-0005) or the non-targeting control siRNA pool (Horizon, #D-001810-10-05) 24 hours after seeding the cells using DharmaFECT 2 (Thermo Scientific, #T-2002-03) as per the manufacturer's instructions. To maintain the knockdown over a 6-day period, at 72 hours post transfection the cells were harvested, split at a ratio of 1:2 into two new wells, and reverse-transfected with siRNA. The cells were then incubated for a further 72 hours before collection.

Quantitative Real-Time PCR (qRT-PCR)

RNA was extracted with TRIzol reagent (Thermo Scientific, #15596026), according to the manufacturer's protocol. The RNA was re-suspended in 30 ul of nuclease-free water and quantified on the NanoDrop spectrophotometer (Thermo Scientific). cDNA synthesis was carried out with 500 ng of RNA using the SensiFAST cDNA Synthesis Kit (Bioline, #BIO-65054) according to the manufacturer's instructions.

qRT-PCR was carried out on the CFX384 Touch Real-Time PCR Detection System (Bio-Rad). A master mix was made for each qRT-PCR target containing 5 ul of KAPA Universal SYBR Fast PCR mix (KAPA Biosystems, #KK4602), 0.6ul of 5 uM forward primer, 0.6 ul of 5 uM reverse primer and 1.8 ul of nuclease free water per reaction. Reactions conditions were 95°C for 3 minutes, followed by 45x cycles of 95 ^{o}C for 3 seconds and 60 ^{o}C for 30 seconds, then a melt curve analysis (65 ^{o}C to 95 ^{o}C, increasing at a rate of 0.5 ^{o}C every 5secs). Primers to detect *SMARCA4* were CAGAACGCACAGACCTTCAA (forward) and

TCACTCTCCTCGCCTTCACT (reverse) and for detection of *18S* GGGACTTAATCAACGCAAGC (forward) and GCAATTATTCCCCATGAACG (reverse). Relative gene expression was calculated using ddCt and normalised to *18S*. A significant change in gene expression of *SMARCA4* between PrEC, LNCaP and PC3 cells was determined by one-way ANOVA and corrected with Tukey's test for multiple comparisons.

Western Blot

Whole cell lysates were collected with lysis buffer (50 mM HEPES, 150 mM NaCl, 10% Glycerol, 1 % Triton-X-100, 1.5 mM $MgCl_2$, 1 mM EGTA, 10 mM Pyrophosphate, 100 mM NaF, Roche protease inhibitor cocktail 1x), and protein level quantified using the Pierce BCA Assay Kit (Thermo Scientific, #23227) according to the manufacturer's instructions. Sample reducing agent (Thermo Scientific, NP0004), loading buffer (Thermo Scientific, NP0007) and 10 ug protein were combined with water to a final volume of 25 ul. Protein samples were heated at 90 ^{o}C for 5 minutes then allowed to cool to room temperature. Protein samples were loaded on a NuPage Novex Bis-Tris 4-12 % gel (Thermo Scientific, NP0321BOX) and electrophoresed at 100V for 1.5 hours in a 1x MOPS buffer (50 mM MOPS (Biochemicals Astral Scientific, #BIOMB03600, 50 mM Tris base, 0.1% SDS, 1 mM EDTA [pH 7.7]). Proteins were transferred to a polyvinylidene fluoride membrane (Bio-Rad, #1620177) at 30 volts for 1 hour using 1x transfer buffer (25 mM Tris base, 192 mM Glycine [pH 8.3]) with 10 % methanol (Sigma-Aldrich, #322415). Membranes were blocked for 1 hour with 5 % skim milk in TBS-T (20 mM Tris, 150 mM NaCl, 0.1% Tween 20 [pH 7.6]) at 4°C. Primary antibodies used were BRG1 (Santa Cruz, sc-10768X) and GAPDH (Ambion, AM4300), which were incubated on samples overnight at 4 ^{o}C with rotation. The membrane was then washed three times for 10mins each in TBS-T with rotation. Secondary antibodies goat anti-mouse (Santa Cruz, sc-2005) and goat anti-rabbit (Santa Cruz, sc-2004) were diluted in TBS-T containing 5 % skim milk and incubated at 4 ^{o}C with rotation for 1 hour. The membrane was washed three times for 10 minutes in TBS-T.

The membrane was then covered with ECL solution (Perkin Elmer, #NEL104001EA), incubated for 1min at room temperature, and visualized by X-ray film. Adjusted relative density calculations were processed through ImageJ (Schneider et al. 2012; Rueden et al. 2017).

Flow cytometric cell cycle analysis

LNCaP cells were seeded at 1.5 x 10^6 cells per 10 cm dish and transfected with siRNA as described. At 72 and 144 hours post transfection the cells were treated with 10 uM EdU for 30 minutes. Remaining EdU was washed off the cells with PBS before harvesting cells, then 1 x 10^6 cells were fixed in 70 % ethanol and frozen at -20 ^{o}C. Cells were then diluted 1 in 4 with PBS then pelleted and re-suspended in 1 ml of PBS containing 1 % BSA (Sigma-Aldrich, #A2058). Cells were again pelleted, re-suspended in 500 ul of click reaction mix (10uM carbocyfluorescine TEG-azide, 10 mM Sodium L-ascorbate, and 2 mM Copper-II-sulphate diluted in PBS), and incubated in the dark at room temperature for 30 minutes. Samples were then diluted with 5 mls of PBS containing 1 % BSA and 0.1 % Tween-20. Cells were again pelleted, washed with PBS and then resuspended in 500 ul of PBS containing 1% BSA, 0.1 mg/ml of RNase and 1 ug/ml of DAPI. Samples were analyised on the Canto II (BD Biosciences). Forward and side scatter were used to select a population of cells free of cell debris and doublets. Cells were analysed using B450 (FTIC – EdU positive) and B510 (DAPI) lasers. 50,000 single cell events were recorded for each ample. FlowJo software v10.5, was used to analyse the data. Data was collected in biological duplicate.

RNA-seq Experiments

Total RNA was extracted with TRIzol reagent, quantified on the Qubit and quality assessed with the Bioanalyzer. An aliquot of 500 ng of total RNA was spiked with external controls ERCC RNA spike-in Mix (Thermo Scientific, 4456740) and libraries constructed with the TruSeq Stranded mRNA sample preparation kit (Illumina, 20020594) according to the manufacturer's

protocol. mRNA Libraries were quantified on Qubit and then stored at -20 ^{o}C. Library quality and fragment size of RNA-seq libraries was assessed on the Bioanalyzer, then KAPA Library Quantification (KAPA Biosystems, #KK4824) was performed according to the manufacturer's protocol. The KAPA quantification results were used to dilute the libraries to 2 nM for sequencing. RNA-seq samples were sequenced for 100 cycles of paired-end reads on the Illumina HiSeq 2500 platform, with four samples multiplexed per lane of the high output run.

RNA-seq Data Analysis

RNA-seq data was processed as described in Taberlay & Achinger-Kawecka *et al.* (Taberlay et al. 2016). Briefly, read counts were normalized with ERCC spike in controls, mapped to hg19/GRCh37 using STAR and counted into genes using the featureCounts (Liao et al. 2014) program. GENCODE v19 was used as a reference transcriptome to determine the transcript per million read (TPM) value. Fold change was calculated within each time point as the log2 ratio of normalized reads per gene using the *edgeR* package in R. Genes with a fold change of ± 1.5 and FDR < 0.01 were considered significantly different. Volcano plots of differential expression were created in R with *ggplots2* and heatmaps with the *heatmap2* package with normalised row Z-score. PCA was performed in R using the *edgeR* package with log counts per million (logCPMS) over GENCODE v19 annotated gene coordinates and normalizing the read counts to library size. RNA-seq multivariate analysis of transcript splicing (MATS) to calculate exon skipping and intron retention was performed with the MATS python package v4.0.2 (Shen et al. 2012; Park et al. 2013; Shen et al. 2014). Transcription factor and GO term enrichment was obtained from Enrichr (http://amp.pharm.mssm.edu/Enrichr/) online gene list analysis tool (Chen et al. 2013; Kuleshov et al. 2016).

TCGA and prostate cell line expression analysis

Pre-processed RNA-seq data from the TCGA prostate adenocarcinoma cohort was downloaded

(cancergenome.nih.gov) for both normal and tumour samples. The average of tumour (n = 486) and normal (n = 52) samples was calculated to determine mean expression. Separation of tumours by Gleason score and molecular subtype was performed in R using the associated clinical data to subset the appropriate groups. Significance was calculated for tumour versus normal using an unpaired T-test. For comparison between Gleason score or molecular subtype, significance was calculated using one-way ANOVA with Dunnett's multiple comparison correction.

Expression data for prostate cell lines from Presner et al. (Prensner et al. 2011) was downloaded from http://www.betastasis.com/prostate_cancer/. Significance between normal, cancer and transformed cell lines was calculated using one-way ANOVA with Dunnett's multiple comparison correction.

ChIP-seq data

The following LNCaP ChIP-seq data was obtained from GEO (ncbi.nlm.nih.gov/geo/); BRG1 accession GSE72690 (Ye et al. 2016), H3K4me3 and H3K27me3 accession GSE38685 (Bert et al. 2013), H3K27ac and H3K4me1 accession GSE73785 (Taberlay et al. 2016). These data were processed through NGSane pipeline as previously described (Bert et al. 2013; Taberlay et al. 2016). Pre-processed bigwig files for FOXA1 and AR were obtained from GEO accession GSE114274 (Gui et al. 2019). Genome browser images of ChIP-seq data were taken from IGV. Heatmaps of ChIP-seq signal were created with *deeptools* (Ramirez et al. 2016).

DATA ACCESS

The BRG1 knockdown RNAseq data generated for this study has been submitted to GEO, accession number GSE150252. Reviewer access for the submitted data is available from;

https://www.ncbi.nlm.nih.gov/geo/query/acc.cgi?acc=GSE150252

ACKNOWLEDGEMENTS

We thank Suat Dervish and the Westmead Flow Cytometry facility for the FACS analysis infrastructure. This work is supported by grants awarded to A.J.C, S.J.C and P.C.T. A.J.C. is supported by grants from the NHMRC (1162886, 1185870), the Goodridge Foundation and the Neil and Norma Hill Foundation. S.J.C. is supported by grants (1011447, 1070418, 1051757) and a fellowship (1156408) from the NHMRC. P.C.T. is supported by project grants from the Cure Cancer Australia Foundation (1060713) and the NHMRC (1051757, 1161985), and a fellowship (1109696) and investigator grant from the NHMRC (1176417).

DISCLOSURE DECLARATION

The authors declare that they have no competing interests. The manuscript has been approved by all authors.

REFERENCES

Agaimy A, Fuchs F, Moskalev EA, Sirbu H, Hartmann A, Haller F. 2017. SMARCA4-deficient pulmonary adenocarcinoma: clinicopathological, immunohistochemical, and molecular characteristics of a novel aggressive neoplasm with a consistent TTF1(neg)/CK7(pos)/HepPar-1(pos) immunophenotype. *Virchows Arch* **471**: 599-609.

Alver BH, Kim KH, Lu P, Wang X, Manchester HE, Wang W, Haswell JR, Park PJ, Roberts CW. 2017. The SWI/SNF chromatin remodelling complex is required for maintenance of lineage specific enhancers. *Nat Commun* **8**: 14648.

Andersson R, Enroth S, Rada-Iglesias A, Wadelius C, Komorowski J. 2009. Nucleosomes are well positioned in exons and carry characteristic histone modifications. *Genome Res* **19**: 1732-1741.

Andreu-Vieyra C, Lai J, Berman BP, Frenkel B, Jia L, Jones PA, Coetzee GA. 2011. Dynamic nucleosome-depleted regions at androgen receptor enhancers in the absence of ligand in prostate cancer cells. *Mol Cell Biol* **31**: 4648-4662.

Bai J, Mei P, Zhang C, Chen F, Li C, Pan Z, Liu H, Zheng J. 2013. BRG1 is a prognostic marker and potential therapeutic target in human breast cancer. *PLoS One* **8**: e59772.

Bao X, Rubin AJ, Qu K, Zhang J, Giresi PG, Chang HY, Khavari PA. 2015. A novel ATAC-seq approach reveals lineage-specific reinforcement of the open chromatin landscape via cooperation between BAF and p63. *Genome biology* **16**: 284.

Barutcu AR, Lajoie BR, Fritz AJ, McCord RP, Nickerson JA, van Wijnen AJ, Lian JB, Stein JL, Dekker J, Stein GS et al. 2016. SMARCA4 regulates gene expression and higher-order chromatin structure in proliferating mammary epithelial cells. *Genome Res* **26**: 1188-1201.

Bert SA, Robinson MD, Strbenac D, Statham AL, Song JZ, Hulf T, Sutherland RL, Coolen MW, Stirzaker C, Clark SJ. 2013. Regional activation of the cancer genome by long-range epigenetic remodeling. *Cancer cell* **23**: 9-22.

Bosse T, ter Haar NT, Seeber LM, v Diest PJ, Hes FJ, Vasen HF, Nout RA, Creutzberg CL, Morreau H, Smit VT. 2013. Loss of ARID1A expression and its relationship with PI3K-Akt pathway alterations, TP53 and microsatellite instability in endometrial cancer. *Modern pathology : an official journal of the United States and Canadian Academy of Pathology, Inc* **26**: 1525-1535.

Bossen C, Murre CS, Chang AN, Mansson R, Rodewald HR, Murre C. 2015. The chromatin remodeler Brg1 activates enhancer repertoires to establish B cell identity and modulate cell growth. *Nat Immunol* **16**: 775-784.

Buscarlet M, Krasteva V, Ho L, Simon C, Hebert J, Wilhelm B, Crabtree GR, Sauvageau G, Thibault P, Lessard JA. 2014. Essential role of BRG, the ATPase subunit of BAF chromatin remodeling complexes, in leukemia maintenance. *Blood* doi:10.1182/blood-2013-02-483495.

Cancer Genome Atlas Research N. 2015. The Molecular Taxonomy of Primary Prostate Cancer. *Cell* **163**: 1011-1025.

Chen EY, Tan CM, Kou Y, Duan Q, Wang Z, Meirelles GV, Clark NR, Ma'ayan A. 2013. Enrichr: interactive and collaborative HTML5 gene list enrichment analysis tool. *BMC Bioinformatics* **14**: 128.

Chen Z, Lan X, Thomas-Ahner JM, Wu D, Liu X, Ye Z, Wang L, Sunkel B, Grenade C, Chen J et al. 2015. Agonist and antagonist switch DNA motifs recognized by human androgen receptor in prostate cancer. *EMBO J* **34**: 502-516.

Chi Y, Senyuk V, Chakraborty S, Nucifora G. 2003. EVI1 promotes cell proliferation by interacting with BRG1 and blocking the repression of BRG1 on E2F1 activity. *J Biol Chem* **278**: 49806-49811.

Cho H, Kim JS, Chung H, Perry C, Lee H, Kim JH. 2013. Loss of ARID1A/BAF250a expression is linked to tumor progression and adverse prognosis in cervical cancer. *Human pathology* **44**: 1365-1374.

Chu X, Guo X, Jiang Y, Yu H, Liu L, Shan W, Yang ZQ. 2017. Genotranscriptomic meta-analysis of the CHD family chromatin remodelers in human cancers - initial evidence of an oncogenic role for CHD7. *Mol Oncol* **11**: 1348-1360.

Church M, Smith KC, Alhussain MM, Pennings S, Fleming AB. 2017. Sas3 and Ada2(Gcn5)-dependent histone H3 acetylation is required for transcription elongation at the de-repressed FLO1 gene. *Nucleic Acids Res* **45**: 4413-4430.

Dai Y, Ngo D, Jacob J, Forman LW, Faller DV. 2008. Prohibitin and the SWI/SNF ATPase subunit BRG1 are required for effective androgen antagonist-mediated transcriptional repression of androgen receptor-regulated genes. *Carcinogenesis* **29**: 1725-1733.

David A, Mabjeesh N, Azar I, Biton S, Engel S, Bernstein J, Romano J, Avidor Y, Waks T, Eshhar Z et al. 2002. Unusual alternative splicing within the human kallikrein genes KLK2 and KLK3 gives rise to novel prostate-specific proteins. *J Biol Chem* **277**: 18084-18090.

Dhami P, Saffrey P, Bruce AW, Dillon SC, Chiang K, Bonhoure N, Koch CM, Bye J, James K, Foad NS et al. 2010. Complex exon-intron marking by histone modifications is not determined solely by nucleosome distribution. *PLoS One* **5**: e12339.

Ding Y, Li N, Dong B, Guo W, Wei H, Chen Q, Yuan H, Han Y, Chang H, Kan S et al. 2019. Chromatin remodeling ATPase BRG1 and PTEN are synthetic lethal in prostate cancer. *J Clin Invest* **129**: 759-773.

Dunaief JL, Strober BE, Guha S, Khavari PA, Alin K, Luban J, Begemann M, Crabtree GR, Goff SP. 1994. The retinoblastoma protein and BRG1 form a complex and cooperate to induce cell cycle arrest. *Cell* **79**: 119-130.

Giles KA, Gould CM, Du Q, Skvortsova K, Song JZ, Maddugoda MP, Achinger-Kawecka J, Stirzaker C, Clark SJ, Taberlay PC. 2019. Integrated epigenomic analysis stratifies chromatin remodellers into distinct functional groups. *Epigenetics Chromatin* **12**: 12.

Giles KA, Taberlay PC. 2019a. Mutations in Chromatin Remodeling Factors. *Encyclopedia of Cancer (Third Edition)* doi:doi.org/10.1016/B978-0-12-801238-3.65225-X: 511-527.

Giles KA, Taberlay PC. 2019b. The Role of Nucleosomes in Epigenetic Gene Regulation. *Clinical Epigenetics*: 87-117.

Gui B, Gui F, Takai T, Feng C, Bai X, Fazli L, Dong X, Liu S, Zhang X, Zhang W et al. 2019. Selective targeting of PARP-2 inhibits androgen receptor signaling and prostate cancer growth through disruption of FOXA1 function. *Proc Natl Acad Sci U S A* **116**: 14573-14582.

Heintzman ND, Stuart RK, Hon G, Fu Y, Ching CW, Hawkins RD, Barrera LO, Van Calcar S, Qu C, Ching KA et al. 2007. Distinct and predictive chromatin signatures of transcriptional promoters and enhancers in the human genome. *Nat Genet* **39**: 311-318.

Herpel E, Rieker RJ, Dienemann H, Muley T, Meister M, Hartmann A, Warth A, Agaimy A. 2017. SMARCA4 and SMARCA2 deficiency in non-small cell lung cancer: immunohistochemical survey of 316 consecutive specimens. *Ann Diagn Pathol* **26**: 47-51.

Hodges HC, Stanton BZ, Cermakova K, Chang CY, Miller EL, Kirkland JG, Ku WL, Veverka V, Zhao K, Crabtree GR. 2018. Dominant-negative SMARCA4 mutants alter the accessibility landscape of tissue-unrestricted enhancers. *Nat Struct Mol Biol* **25**: 61-72.

Hoffman JA, Trotter KW, Ward JM, Archer TK. 2018. BRG1 governs glucocorticoid receptor interactions with chromatin and pioneer factors across the genome. *Elife* **7**.

Hu G, Schones DE, Cui K, Ybarra R, Northrup D, Tang Q, Gattinoni L, Restifo NP, Huang S, Zhao K. 2011. Regulation of nucleosome landscape and transcription factor targeting at tissue-specific enhancers by BRG1. *Genome Res* **21**: 1650-1658.

Hu Z, Chen K, Xia Z, Chavez M, Pal S, Seol JH, Chen CC, Li W, Tyler JK. 2014. Nucleosome loss leads to global transcriptional up-regulation and genomic instability during yeast aging. *Genes Dev* **28**: 396-408.

Huang H, Yu S, Liu H, Sun X. 2012. Nucleosome organization in sequences of alternative events in human genome. *Bio Systems* **109**: 214-219.

Jones D, Wade M, Nakjang S, Chaytor L, Grey J, Robson CN, Gaughan L. 2015. FOXA1 regulates androgen receptor variant activity in models of castrate-resistant prostate cancer. *Oncotarget* **6**: 29782-29794.

Kadoch C, Hargreaves DC, Hodges C, Elias L, Ho L, Ranish J, Crabtree GR. 2013. Proteomic and bioinformatic analysis of mammalian SWI/SNF complexes identifies extensive roles in human malignancy. *Nat Genet* **45**: 592-601.

Katagiri A, Nakayama K, Rahman MT, Rahman M, Katagiri H, Nakayama N, Ishikawa M, Ishibashi T, Iida K, Kobayashi H et al. 2012. Loss of ARID1A expression is related to shorter progression-free survival and chemoresistance in ovarian clear cell carcinoma. *Modern pathology : an official journal of the United States and Canadian Academy of Pathology, Inc* **25**: 282-288.

Kaufmann B, Wang B, Zhong S, Laschinger M, Patil P, Lu M, Assfalg V, Cheng Z, Friess H, Huser N et al. 2017. BRG1 promotes hepatocarcinogenesis by regulating proliferation and invasiveness. *PLoS One* **12**: e0180225.

Kim SI, Bresnick EH, Bultman SJ. 2009a. BRG1 directly regulates nucleosome structure and chromatin looping of the alpha globin locus to activate transcription. *Nucleic Acids Res* **37**: 6019-6027.

Kim SI, Bultman SJ, Kiefer CM, Dean A, Bresnick EH. 2009b. BRG1 requirement for long-range interaction of a locus control region with a downstream promoter. *Proc Natl Acad Sci U S A* **106**: 2259-2264.

Kuleshov MV, Jones MR, Rouillard AD, Fernandez NF, Duan Q, Wang Z, Koplev S, Jenkins SL, Jagodnik KM, Lachmann A et al. 2016. Enrichr: a comprehensive gene set enrichment analysis web server 2016 update. *Nucleic Acids Res* **44**: W90-97.

Leung JY, Nevins JR. 2012. E2F6 associates with BRG1 in transcriptional regulation. *PLoS One* **7**: e47967.

Li XY, Thomas S, Sabo PJ, Eisen MB, Stamatoyannopoulos JA, Biggin MD. 2011. The role of chromatin accessibility in directing the widespread, overlapping patterns of Drosophila transcription factor binding. *Genome Biol* **12**: R34.

Li Y, Shi QL, Jin XZ, Meng K, Zhou XJ, Sun LP. 2006. [BRG1 expression in prostate carcinoma by application of tissue microarray]. *Zhonghua Nan Ke Xue* **12**: 629-632.

Liao Y, Smyth GK, Shi W. 2014. featureCounts: an efficient general purpose program for assigning sequence reads to genomic features. *Bioinformatics* **30**: 923-930.

Lin KT, Gong J, Li CF, Jang TH, Chen WL, Chen HJ, Wang LH. 2012. Vav3-rac1 signaling regulates prostate cancer metastasis with elevated Vav3 expression correlating with prostate cancer progression and posttreatment recurrence. *Cancer Res* **72**: 3000-3009.

Liu XB, Sun AJ, Wang C, Chen LR. 2010. [Expression of BRG1 and BRM proteins in prostatic cancer]. *Zhonghua Bing Li Xue Za Zhi* **39**: 591-594.

Liu Y, Mo JQ, Hu Q, Boivin G, Levin L, Lu S, Yang D, Dong Z, Lu S. 2008. Targeted overexpression of vav3 oncogene in prostatic epithelium induces nonbacterial prostatitis and prostate cancer. *Cancer Res* **68**: 6396-6406.

Luebben WR, Sharma N, Nyborg JK. 2010. Nucleosome eviction and activated transcription require p300 acetylation of histone H3 lysine 14. *Proc Natl Acad Sci U S A* **107**: 19254-19259.

Lyons LS, Burnstein KL. 2006. Vav3, a Rho GTPase guanine nucleotide exchange factor, increases during progression to androgen independence in prostate cancer cells and potentiates androgen receptor transcriptional activity. *Mol Endocrinol* **20**: 1061-1072.

Makova KD, Hardison RC. 2015. The effects of chromatin organization on variation in mutation rates in the genome. *Nat Rev Genet* **16**: 213-223.

Mao TL, Ardighieri L, Ayhan A, Kuo KT, Wu CH, Wang TL, Shih Ie M. 2013. Loss of ARID1A expression correlates with stages of tumor progression in uterine endometrioid carcinoma. *The American journal of surgical pathology* **37**: 1342-1348.

Marshall TW, Link KA, Petre-Draviam CE, Knudsen KE. 2003. Differential requirement of SWI/SNF for androgen receptor activity. *J Biol Chem* **278**: 30605-30613.

Medina PP, Romero OA, Kohno T, Montuenga LM, Pio R, Yokota J, Sanchez-Cespedes M. 2008. Frequent BRG1/SMARCA4-inactivating mutations in human lung cancer cell lines. *Hum Mutat* **29**: 617-622.

Morrison EA, Sanchez JC, Ronan JL, Farrell DP, Varzavand K, Johnson JK, Gu BX, Crabtree GR, Musselman CA. 2017. DNA binding drives the association of BRG1/hBRM bromodomains with nucleosomes. *Nat Commun* **8**: 16080.

Muthuswami R, Bailey L, Rakesh R, Imbalzano AN, Nickerson JA, Hockensmith JW. 2019. BRG1 is a prognostic indicator and a potential therapeutic target for prostate cancer. *J Cell Physiol* doi:10.1002/jcp.28161.

Naidu SR, Love IM, Imbalzano AN, Grossman SR, Androphy EJ. 2009. The SWI/SNF chromatin remodeling subunit BRG1 is a critical regulator of p53 necessary for proliferation of malignant cells. *Oncogene* **28**: 2492-2501.

Ni Z, Abou El Hassan M, Xu Z, Yu T, Bremner R. 2008. The chromatin-remodeling enzyme BRG1 coordinates CIITA induction through many interdependent distal enhancers. *Nat Immunol* **9**: 785-793.

O'Sullivan RJ, Kubicek S, Schreiber SL, Karlseder J. 2010. Reduced histone biosynthesis and chromatin changes arising from a damage signal at telomeres. *Nat Struct Mol Biol* **17**: 1218-1225.

Oike T, Ogiwara H, Nakano T, Yokota J, Kohno T. 2013a. Inactivating mutations in SWI/SNF chromatin remodeling genes in human cancer. *Jpn J Clin Oncol* **43**: 849-855.

Oike T, Ogiwara H, Tominaga Y, Ito K, Ando O, Tsuta K, Mizukami T, Shimada Y, Isomura H, Komachi M et al. 2013b. A synthetic lethality-based strategy to treat cancers harboring a genetic deficiency in the chromatin remodeling factor BRG1. *Cancer Res* **73**: 5508-5518.

Park JW, Tokheim C, Shen S, Xing Y. 2013. Identifying differential alternative splicing events from RNA sequencing data using RNASeq-MATS. *Methods Mol Biol* **1038**: 171-179.

Pomerantz MM, Li F, Takeda DY, Lenci R, Chonkar A, Chabot M, Cejas P, Vazquez F, Cook J, Shivdasani RA et al. 2015. The androgen receptor cistrome is extensively reprogrammed in human prostate tumorigenesis. *Nat Genet* **47**: 1346-1351.

Prensner JR, Chen W, Han S, Iyer MK, Cao Q, Kothari V, Evans JR, Knudsen KE, Paulsen MT, Ljungman M et al. 2014. The long non-coding RNA PCAT-1 promotes prostate cancer cell proliferation through cMyc. *Neoplasia* **16**: 900-908.

Prensner JR, Iyer MK, Balbin OA, Dhanasekaran SM, Cao Q, Brenner JC, Laxman B, Asangani IA, Grasso CS, Kominsky HD et al. 2011. Transcriptome sequencing across a prostate cancer cohort identifies PCAT-1, an unannotated lincRNA implicated in disease progression. *Nat Biotechnol* **29**: 742-749.

Ramirez F, Ryan DP, Gruning B, Bhardwaj V, Kilpert F, Richter AS, Heyne S, Dundar F, Manke T. 2016. deepTools2: a next generation web server for deep-sequencing data analysis. *Nucleic Acids Res* **44**: W160-165.

Ramirez-Carrozzi VR, Braas D, Bhatt DM, Cheng CS, Hong C, Doty KR, Black JC, Hoffmann A, Carey M, Smale ST. 2009. A unifying model for the selective regulation of inducible transcription by CpG islands and nucleosome remodeling. *Cell* **138**: 114-128.

Rao S, Lyons LS, Fahrenholtz CD, Wu F, Farooq A, Balkan W, Burnstein KL. 2012. A novel nuclear role for the Vav3 nucleotide exchange factor in androgen receptor coactivation in prostate cancer. *Oncogene* **31**: 716-727.

Reisman D, Glaros S, Thompson EA. 2009. The SWI/SNF complex and cancer. *Oncogene* **28**: 1653-1668.

Roberts CW, Biegel JA. 2009. The role of SMARCB1/INI1 in development of rhabdoid tumor. *Cancer biology & therapy* **8**: 412-416.

Roberts CW, Orkin SH. 2004. The SWI/SNF complex--chromatin and cancer. *Nat Rev Cancer* **4**: 133-142.

Romero OA, Torres-Diz M, Pros E, Savola S, Gomez A, Moran S, Saez C, Iwakawa R, Villanueva A, Montuenga LM et al. 2013. MAX inactivation in small-cell lung cancer disrupts the MYC-SWI/SNF programs and is synthetic lethal with BRG1. *Cancer discovery* doi:10.1158/2159-8290.cd-13-0799.

Roy DM, Walsh LA, Chan TA. 2014. Driver mutations of cancer epigenomes. *Protein Cell* **5**: 265-296.

Rueden CT, Schindelin J, Hiner MC, DeZonia BE, Walter AE, Arena ET, Eliceiri KW. 2017. ImageJ2: ImageJ for the next generation of scientific image data. *BMC Bioinformatics* **18**: 529.

Schneider CA, Rasband WS, Eliceiri KW. 2012. NIH Image to ImageJ: 25 years of image analysis. *Nat Methods* **9**: 671-675.

Shain AH, Pollack JR. 2013. The spectrum of SWI/SNF mutations, ubiquitous in human cancers. *PLoS One* **8**: e55119.

Shang Z, Niu Y, Cai Q, Chen J, Tian J, Yeh S, Lai KP, Chang C. 2014. Human kallikrein 2 (KLK2) promotes prostate cancer cell growth via function as a modulator to promote the ARA70-enhanced androgen receptor transactivation. *Tumour Biol* **35**: 1881-1890.

Shang Z, Yu J, Sun L, Tian J, Zhu S, Zhang B, Dong Q, Jiang N, Flores-Morales A, Chang C et al. 2019. LncRNA PCAT1 activates AKT and NF-kappaB signaling in castration-resistant prostate cancer by regulating the PHLPP/FKBP51/IKKalpha complex. *Nucleic Acids Res* **47**: 4211-4225.

Shen S, Park JW, Huang J, Dittmar KA, Lu ZX, Zhou Q, Carstens RP, Xing Y. 2012. MATS: a Bayesian framework for flexible detection of differential alternative splicing from RNA-Seq data. *Nucleic Acids Res* **40**: e61.

Shen S, Park JW, Lu ZX, Lin L, Henry MD, Wu YN, Zhou Q, Xing Y. 2014. rMATS: robust and flexible detection of differential alternative splicing from replicate RNA-Seq data. *Proc Natl Acad Sci U S A* **111**: E5593-5601.

Shen W, Xu C, Huang W, Zhang J, Carlson JE, Tu X, Wu J, Shi Y. 2007. Solution structure of human Brg1 bromodomain and its specific binding to acetylated histone tails. *Biochemistry* **46**: 2100-2110.

Shi J, Whyte WA, Zepeda-Mendoza CJ, Milazzo JP, Shen C, Roe JS, Minder JL, Mercan F, Wang E, Eckersley-Maslin MA et al. 2013. Role of SWI/SNF in acute leukemia maintenance and enhancer-mediated Myc regulation. *Genes Dev* **27**: 2648-2662.

Skulte KA, Phan L, Clark SJ, Taberlay PC. 2014. Chromatin remodeler mutations in human cancers: epigenetic implications. *Epigenomics* **6**: 397-414.

Song S, Walter V, Karaca M, Li Y, Bartlett CS, Smiraglia DJ, Serber D, Sproul CD, Plass C, Zhang J et al. 2014. Gene Silencing Associated with SWI/SNF Complex Loss During NSCLC Development. *Molecular cancer research : MCR* doi:10.1158/1541-7786.mcr-13-0427.

Stelloo S, Nevedomskaya E, Kim Y, Hoekman L, Bleijerveld OB, Mirza T, Wessels LFA, van Weerden WM, Altelaar AFM, Bergman AM et al. 2018. Endogenous androgen receptor proteomic profiling reveals genomic subcomplex involved in prostate tumorigenesis. *Oncogene* **37**: 313-322.

Strobeck MW, Knudsen KE, Fribourg AF, DeCristofaro MF, Weissman BE, Imbalzano AN, Knudsen ES. 2000. BRG-1 is required for RB-mediated cell cycle arrest. *Proc Natl Acad Sci U S A* **97**: 7748-7753.

Strober BE, Dunaief JL, Guha, Goff SP. 1996. Functional interactions between the hBRM/hBRG1 transcriptional activators and the pRB family of proteins. *Mol Cell Biol* **16**: 1576-1583.

Sun A, Tawfik O, Gayed B, Thrasher JB, Hoestje S, Li C, Li B. 2007. Aberrant expression of SWI/SNF catalytic subunits BRG1/BRM is associated with tumor development and increased invasiveness in prostate cancers. *Prostate* **67**: 203-213.

Taberlay PC, Achinger-Kawecka J, Lun AT, Buske FA, Sabir K, Gould CM, Zotenko E, Bert SA, Giles KA, Bauer DC et al. 2016. Three-dimensional disorganization of the cancer genome occurs coincident with long-range genetic and epigenetic alterations. *Genome Res* **26**: 719-731.

Taberlay PC, Statham AL, Kelly TK, Clark SJ, Jones PA. 2014. Reconfiguration of nucleosome-depleted regions at distal regulatory elements accompanies DNA methylation of enhancers and insulators in cancer. *Genome Res* **24**: 1421-1432.

Tagal V, Wei S, Zhang W, Brekken RA, Posner BA, Peyton M, Girard L, Hwang T, Wheeler DA, Minna JD et al. 2017. SMARCA4-inactivating mutations increase sensitivity to Aurora kinase A inhibitor VX-680 in non-small cell lung cancers. *Nat Commun* **8**: 14098.

Thurman RE, Rynes E, Humbert R, Vierstra J, Maurano MT, Haugen E, Sheffield NC, Stergachis AB, Wang H, Vernot B et al. 2012. The accessible chromatin landscape of the human genome. *Nature* **489**: 75-82.

Tolstorukov MY, Sansam CG, Lu P, Koellhoffer EC, Helming KC, Alver BH, Tillman EJ, Evans JA, Wilson BG, Park PJ et al. 2013. Swi/Snf chromatin remodeling/tumor suppressor complex establishes nucleosome occupancy at target promoters. *Proc Natl Acad Sci U S A* **110**: 10165-10170.

Valdman A, Nordenskjold A, Fang X, Naito A, Al-Shukri S, Larsson C, Ekman P, Li C. 2003. Mutation analysis of the BRG1 gene in prostate cancer clinical samples. *Int J Oncol* **22**: 1003-1007.

Velez-Cruz R, Manickavinayaham S, Biswas AK, Clary RW, Premkumar T, Cole F, Johnson DG. 2016. RB localizes to DNA double-strand breaks and promotes DNA end resection and homologous recombination through the recruitment of BRG1. *Genes Dev* **30**: 2500-2512.

Venkatesh S, Workman JL. 2015. Histone exchange, chromatin structure and the regulation of transcription. *Nature reviews Molecular cell biology* **16**: 178-189.

Vicent GP, Ballare C, Zaurin R, Saragueta P, Beato M. 2006. Chromatin remodeling and control of cell proliferation by progestins via cross talk of progesterone receptor with the estrogen receptors and kinase signaling pathways. *Ann N Y Acad Sci* **1089**: 59-72.

Vieira JM, Howard S, Villa Del Campo C, Bollini S, Dube KN, Masters M, Barnette DN, Rohling M, Sun X, Hankins LE et al. 2017. BRG1-SWI/SNF-dependent regulation of the Wt1 transcriptional landscape mediates epicardial activity during heart development and disease. *Nat Commun* **8**: 16034.

Williams SA, Xu Y, De Marzo AM, Isaacs JT, Denmeade SR. 2010. Prostate-specific antigen (PSA) is activated by KLK2 in prostate cancer ex vivo models and in prostate-targeted PSA/KLK2 double transgenic mice. *Prostate* **70**: 788-796.

Wilson BG, Helming KC, Wang X, Kim Y, Vazquez F, Jagani Z, Hahn WC, Roberts CW. 2014. Residual complexes containing SMARCA2 (BRM) underlie the oncogenic drive of SMARCA4 (BRG1) mutation. *Mol Cell Biol* doi:10.1128/mcb.01372-13.

Wilson BG, Roberts CW. 2011. SWI/SNF nucleosome remodellers and cancer. *Nat Rev Cancer* **11**: 481-492.

Wong AK, Shanahan F, Chen Y, Lian L, Ha P, Hendricks K, Ghaffari S, Iliev D, Penn B, Woodland AM et al. 2000. BRG1, a component of the SWI-SNF complex, is mutated in multiple human tumor cell lines. *Cancer Res* **60**: 6171-6177.

Yan HB, Wang XF, Zhang Q, Tang ZQ, Jiang YH, Fan HZ, Sun YH, Yang PY, Liu F. 2013. Reduced expression of the chromatin remodeling gene ARID1A enhances gastric cancer cell migration and invasion via downregulation of E-cadherin transcription. *Carcinogenesis* doi:10.1093/carcin/bgt398.

Ye Z, Chen Z, Sunkel B, Frietze S, Huang TH, Wang Q, Jin VX. 2016. Genome-wide analysis reveals positional-nucleosome-oriented binding pattern of pioneer factor FOXA1. *Nucleic Acids Res* **44**: 7540-7554.

Yokoyama Y, Matsushita Y, Shigeto T, Futagami M, Mizunuma H. 2014. Decreased ARID1A expression is correlated with chemoresistance in epithelial ovarian cancer. *Journal of gynecologic oncology* **25**: 58-63.

You JS, Jones PA. 2012. Cancer genetics and epigenetics: two sides of the same coin? *Cancer cell* **22**: 9-20.

Zhang HS, Gavin M, Dahiya A, Postigo AA, Ma D, Luo RX, Harbour JW, Dean DC. 2000. Exit from G1 and S phase of the cell cycle is regulated by repressor complexes containing HDAC-Rb-hSWI/SNF and Rb-hSWI/SNF. *Cell* **101**: 79-89.

Zhao J, Liu C, Zhao Z. 2014. ARID1A: a potential prognostic factor for breast cancer. *Tumour Biol* doi:10.1007/s13277-014-1632-7.